Available online at www.sciencedirect.com

SciVerse ScienceDirect

Ceramics International 39 (2013) 8043–8048

CERAMICS INTERNATIONAL

www.elsevier.com/locate/ceramint

A hybrid dielectric resonator antenna based upon novel complex perovskite microwave ceramic

Yih-Chien Chen*, Kuang-Chiung Chang, Da-Yeh Tsai

Department of Electrical Engineering, Lunghwa University of Science and Technology, Gueishan Shiang, Taoyuan County, Taiwan

Received 4 March 2013; received in revised form 19 March 2013; accepted 19 March 2013
Available online 3 April 2013

Abstract

The microwave dielectric properties of $Nd(Mg_{0.5-x}Ca_xSn_{0.5})O_3$ ceramics were examined to evaluate their exploitation in mobile communication. The X-ray diffraction patterns of $Nd(Mg_{0.43}Ca_{0.07}Sn_{0.5})O_3$ ceramics revealed no significant variation of phase with sintering temperatures. $Nd(Mg_{0.43}Ca_{0.07}Sn_{0.5})O_3$ ceramics that were sintered at 1550 °C for 4 h had the following properties: a density of 6.88 g/cm^3, a dielectric constant (ε_r) of 19.51, a quality factor (Qf) of 100,400 GHz, and a temperature coefficient of resonant frequency (τ_f) of −57.8 ppm/°C. The proposed hybrid dielectric resonator covered the industrial, scientific, medical (ISM), high-performance radio local area network (HIPERLAN), and unlicensed national information infrastructure (UNII) bands. A 12.5% bandwidth (return loss < 10 dB) of 2.43 GHz, and a 14.2% bandwidth (return loss < 10 dB) of 5.62 GHz were successfully achieved.
© 2013 Elsevier Ltd and Techna Group S.r.l. All rights reserved.

Keywords: $Nd(Mg_{0.43}Ca_{0.07}Sn_{0.5})O_3$; Dielectric constant; Quality factor; Temperature coefficient of resonant frequency; Dielectric resonator antenna

1. Introduction

Materials that are used in microwave devices must have three dielectric characteristics—a high dielectric constant, a high quality factor, and a near-zero temperature coefficient of resonant frequency [1]. These characteristics enable small devices with low loss and high temperature stability to be fabricated. The benefits of using complex perovskite ceramics are reportedly associated with their excellent microwave dielectric properties. Many investigations of $Nd(Mg_{0.5}Sn_{0.5})O_3$ ceramics have focused on their potential application in resonators, filters, and antennas in modern communication systems, including radars and wireless local area networks, which are operated at microwave frequencies. Previous research on $Nd(Mg_{0.5}Sn_{0.5})O_3$ ceramics that were sintered at 1550 °C for 4 h reported a dielectric constant of 19.3 and a Qf of 43,300 GHz [2]. Additionally, 0.25 wt% B_2O_3-doped $Nd(Mg_{0.5}Sn_{0.5})O_3$ ceramics that were sintered at 1500 °C for 4 h had a dielectric constant of about 18.9 and a Qf of 32,300 GHz [3]. A density of 6.88 g/cm^3, a dielectric constant of 19.3 and a Qf of 91,200 GHz were obtained for $Nd_{2.94/3}Sr_{0.03}(Mg_{0.5}Sn_{0.5})O_3$ ceramics that were sintered at 1550 °C for 4 h [4]. A dielectric constant of 19.5 and a quality factor (Qf) of 129,200 GHz were obtained for $Nd(Mg_{0.4}Zn_{0.1}Sn_{0.5})O_3$ ceramics sintered at 1500 °C for 4 h [5]. A dielectric constant of 21.1 and a Qf of 50,000 GHz were obtained for $Nd(Mg_{0.5}Sn_{0.4}Ti_{0.1})O_3$ ceramics that were sintered at 1550 °C for 4 h [6]. The fact that the ionic radius of Ca^{2+} (0.100 nm) is relatively larger than that of Mg^{2+} (0.072 nm) motivates this study of the effect of the substitution of Mg^{2+} by Ca^{2+} to form $Nd(Mg_{0.5-x}Ca_xSn_{0.5})O_3$ [7].

In this investigation, $Nd(Mg_{0.5-x}Ca_xSn_{0.5})O_3$ ceramics were synthesized, and some of the Mg^{2+} ions were substituted by Ca^{2+} ions to improve their microwave dielectric properties. Moreover, the effect of the sintering temperature on the microwave dielectric properties of $Nd(Mg_{0.5-x}Ca_xSn_{0.5})O_3$ ceramics was investigated. $Nd(Mg_{0.5-x}Ca_xSn_{0.5})O_3$ ceramics were synthesized using the conventional mixed-oxide method and demonstrated better microwave dielectric properties than $Nd(Mg_{0.5}Sn_{0.5})O_3$ ceramics. The microwave dielectric properties of $Nd(Mg_{0.5-x}Ca_xSn_{0.5})O_3$ ceramics were found to vary with the extent of Ca^{2+} substitution and sintering temperature. To further understand these different microwave dielectric properties, the ceramics were further analyzed by densification. In addition, the X-ray diffraction (XRD) patterns and microstructures of the ceramics were analyzed.

*Corresponding author. Tel.: +886 2 8209 3211; fax: +886 2 8209 9728.
E-mail addresses: EE049@mail.lhu.edu.tw, ycchenncku@yahoo.com.tw (Y.-C. Chen).

0272-8842/$ - see front matter © 2013 Elsevier Ltd and Techna Group S.r.l. All rights reserved.
http://dx.doi.org/10.1016/j.ceramint.2013.03.074

Many commercial applications, including mobile radio and wireless communications, use microstrip antennas. However, these microstrip antennas have a limited range of sizes, bandwidth, and efficiency. On the other hand, dielectric resonator (DR) antenna is attractive due to its small-size, high radiation efficiency, and ease of excitation [8]. Many investigations of DR antenna composed of DR with relatively small dielectric constant around 10 have been examined to enhance radiation capability [9–11]. The use of dual band antennas in wireless local area network (WLAN) has been increasing rapidly in the last decade. Dual band antennas were applied in industrial, scientific, medical (ISM, 2.4–2.484 GHz) in low band of WLAN. At the same time, dual band antennas were also applied in high band of WLAN, including high-performance radio local area network (HIPERLAN, 5.15–5.35 GHz), and unlicensed national information infrastructure (UNII, 5.725–5.825 GHz). Dual band DR antennas were implemented by placing a parasitic element near the radiation part, or stacking many DRs. In this paper, the hybrid DR antenna, consisting of a cylindrical high dielectric constant DR and a rectangular slot, operated in the ISM, HIPERLAN, and UNII bands simultaneously. However, the volume of the hybrid DR antenna did not increase. The radiating resonators in the hybrid DR antenna were assembled tightly and resonated at two frequencies. The characteristics of the hybrid DR antenna, such as return loss, radiation pattern, and gain were measured and discussed.

2. Experimental procedure

The starting raw chemicals were highly pure Nd_2O_3 (99.99%), MgO (98.0%), $CaCO_3$ (99.0%), and SnO_2 (99.0%) powders. The prepared composition was $Nd(Mg_{0.5-x}Ca_xSn_{0.5})O_3$ (x=0.05, 0.07, and 0.1). Specimens were prepared using the conventional mixed-oxide method. The starting materials were weighed and used in appropriate molar ratios. The raw material was ball-milled in alcohol for 12 h, dried, and then calcined at 1200 °C for 4 h. The calcined powder was re-milled for 12 h using PVA solution as a binder. The fine powder was then crushed into a finer powder using a sieve with a 200 mesh. The very fine powder thus obtained was then axially pressed at 2000 kg/cm^2 into pellets with a diameter of 11 mm and a thickness of 6 mm. These specimens were then sintered at temperatures of 1450–1600 °C for 4 h in air. Both the heating rate and the cooling rate were set to 10 °C/min.

After sintering, the phases of the samples were investigated by X-ray diffraction. An X-ray Rigaku D/MAX-2200 was used with Cu$K\alpha$ radiation (at 30 kV and 20 mA) and a graphite monochromator in the 2θ range of 10–80°. Scanning electron microscopy (SEM; JEOL JSM-6500F) and energy dispersive X-ray spectrometry (EDS) were utilized to examine the microstructures of the specimens. The apparent densities of the specimens were measured by Archimedes' method in distilled water. The microwave dielectric properties of the specimens were measured by the postresonator method developed by Hakki and Coleman [12]. The value of τ_f was measured by the same method as the dielectric constant. The test cavity was placed in a chamber and the temperature was increased from 25 to 75 °C. The τ_f value (ppm/°C) was determined from the change in resonant frequency,

$$\tau_f = \frac{f_2 - f_1}{f_1(T_2 - T_1)}, \tag{1}$$

where f_1 and f_2 are the resonant frequencies at T_1 and T_2, respectively.

The resonant frequency of the cylindrical DR antenna is

$$f_{110}^{TM} = \frac{c}{2\pi r\sqrt{\varepsilon_{ra}}}\sqrt{X_{11}^{'2} + \left(\frac{\pi r}{2t}\right)^2} \tag{2}$$

where $X_{11}^{'} = 1.841$ is the first zero of the equation $J_1^{'}(x) = 0$, and c is the speed of light in vacuum. The parameters r, t, and ε_{ra} are the radius, height, and dielectric constant of the DR, respectively. Fig. 1 shows the configuration of the proposed hybrid DR antenna, consisting of a rectangular slot and a cylindrical high dielectric constant DR. The rectangular FR4 substrate had dimensions of 50.0 × 50.0 mm^2 and a thickness of 1.6 mm. The cylindrical DR was fed with a microstrip line. The microstrip feed line was placed below the centerline (y-axis in the figure) of the dielectric resonator. Dimensions of the microstrip feed line on FR4 substrate was calculated by close-form formulas, assuming infinite ground plane and finite dielectric thickness. The microstrip feeding line had length L_f of 27.0 mm and width W_f of 6.0 mm. The DR had a dielectric constant ε_{ra}=19.51, radius r=2.5 mm, and height t=5.0 mm. The DR was a low loss ceramic composed of Nd$(Mg_{0.43}Ca_{0.07}Sn_{0.5})O_3$ that was sintered at 1550 °C for 4 h. The rectangular slot on the front side of the FR4 substrate fed with microstrip line, resonated at approximately half guided wavelength, λgs, where λgs was the guided wavelength of the slot. The length of rectangular slot was 33 mm.

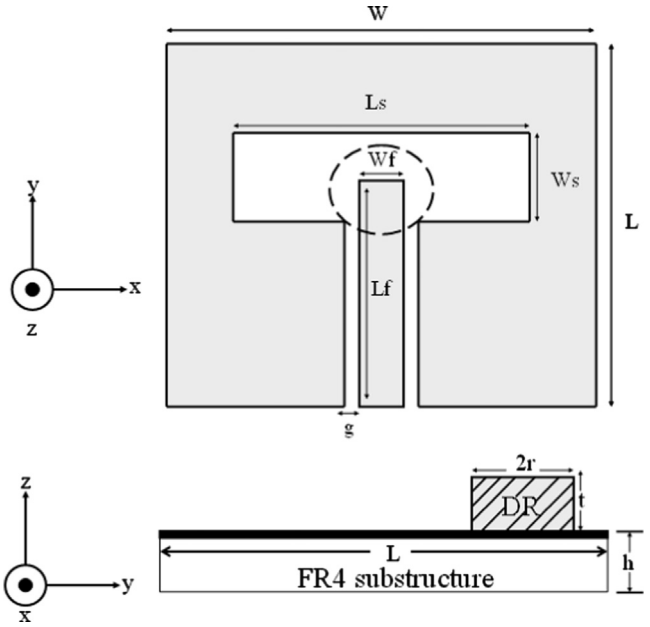

Fig. 1. Configuration of the proposed hybrid DR antenna consisted of a cylindrical high dielectric constant DR and a rectangular slot.

3. Results and discussion

Fig. 2 shows the X-ray diffraction patterns of Nd($Mg_{0.43}Ca_{0.07}Sn_{0.5}$)$O_3$ ceramics sintered at 1450–1600 °C for 4 h. The X-ray diffraction patterns of Nd($Mg_{0.43}Ca_{0.07}Sn_{0.5}$)$O_3$ ceramics did not vary significantly with the sintering temperature. Clearly, Nd($Mg_{0.43}Ca_{0.07}Sn_{0.5}$)$O_3$ was the main crystalline phase, which was accompanied by a small amount of $Nd_2Sn_2O_7$ as the second phase. $Nd_2Sn_2O_7$ with a cubic crystal structure (ICDD-PDF #87-1220) was identified and proved difficult to eliminate completely from samples that were prepared by the mixed oxide route. A later investigation will involve preparing of the powder by precipitation from the solution. This method may yield a single-phase product. A single-phase product potentially has much higher values of the parameters of interest. As displayed in Fig. 2, the (2 2 2) and (4 0 0) peaks of the $Nd_2Sn_2O_7$ second phase were at 29.253° and 33.905°, respectively. All the peaks for Nd($Mg_{0.43}Ca_{0.07}Sn_{0.5}$)$O_3$ ceramics were indexed based on the cubic perovskite unit cell. A series of extra peaks were observed and corresponded to superlattice reflections. All superlattice reflections were indexed using half-integer Miller indices. According to Glazer, superlattice reflections, with specific combinations of odd (*o*) and even (*e*) Miller indices, indicated particular deviations of the structure from the undistorted cubic structure, such as octahedral in-phase tilting (*ooe*, *oeo*, *eoo*), anti-phase tilting (*ooo*, $h+k+l>3$), and anti-parallel displacement of A-cations (*eeo*, *eoe*, *oee*) [13]. The extra (1/2(2 1 0), 1/2(3 0 0), 1/2(3 2 0), 1/2 (4 1 0), 1/2(4 2 1), 1/2 (4 3 2), and 1/2(4 4 1)) peaks demonstrated A-site cation displacement; the (1/2(3 1 1), 1/2(3 3 1), and 1/2(5 1 1)) peaks indicated anti-phase tilting; and the 1/2(3 2 1) peak indicated in-phase tilting. The 1/2(1 1 1) peak provided evidence of 1:1 B-site cation ordering. Nd($Mg_{0.5-x}Ca_xSn_{0.5}$)O_3 ceramics exhibited a decrease in tolerance factor from 0.8944 to 0.8838 as x increased from 0.05 to 0.1. The tolerance factors were calculated using the ionic radius data of Shannon [7]. The tolerance factors for Nd($Mg_{0.5-x}Ca_x$-$Sn_{0.5}$)O_3 ceramics were in the anti-phase and in-phase titled regions [14], which is in agreement with the X-ray diffraction patterns described above.

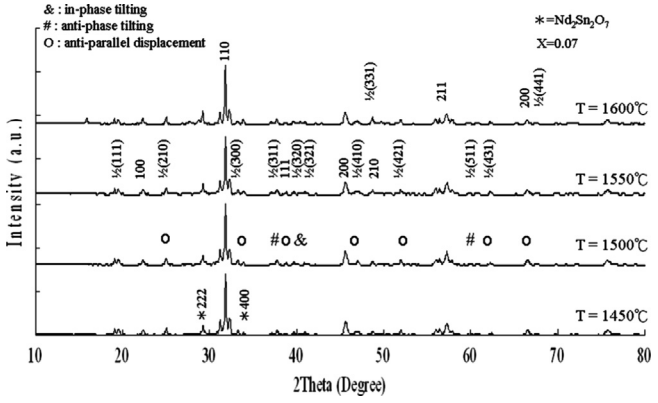

Fig. 2. X-ray diffraction patterns of Nd($Mg_{0.43}Ca_{0.07}Sn_{0.5}$)$O_3$ specimens sintered at 1450–1600 °C for 4 h **(o, anti-parallel displacement; #, anti-phase tilting; &, in-phase tilting).**

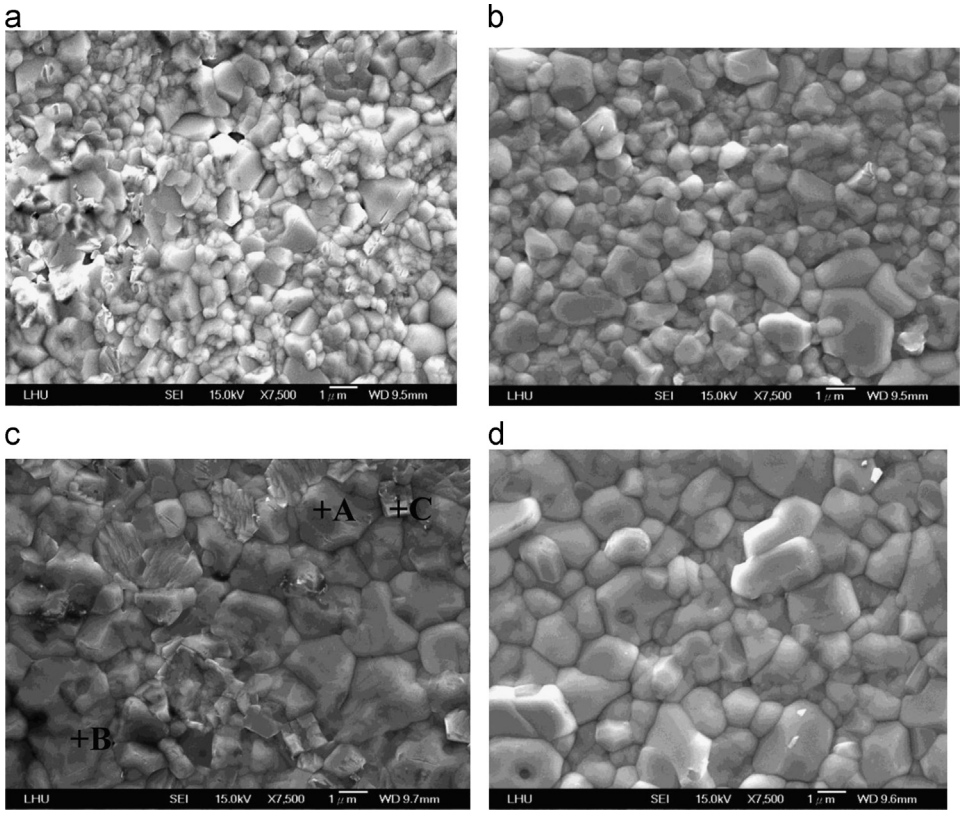

Fig. 3. Microstructures of Nd($Mg_{0.43}Ca_{0.07}Sn_{0.5}$)$O_3$ ceramics sintered at different temperatures for 4 h: (a) 1450 °C, (b) 1500 °C, (c) 1550 °C and (d) 1600 °C.

Fig. 3 shows the microstructures of $Nd(Mg_{0.43}Ca_{0.07}Sn_{0.5})O_3$ ceramics, following sintering for 4 h at various temperatures. $Nd(Mg_{0.43}Ca_{0.07}Sn_{0.5})O_3$ ceramics were not dense, and their grains did not grow after sintering at 1450 °C for 4 h, potentially degrading the microwave dielectric properties of $Nd(Mg_{0.43}Ca_{0.07}Sn_{0.5})O_3$ ceramics. The pores of $Nd(Mg_{0.43}Ca_{0.07}Sn_{0.5})O_3$ ceramics almost disappeared upon sintering at 1550 °C for 4 h. Table 1 shows the porosities of the specimens that were sintered at 1550 °C for 4 h. The porosities of $Nd(Mg_{0.5-x}Ca_xSn_{0.5})O_3$ ceramics were lower than 0.7%. To identify the composition of the second phase, an energy-disperse spectroscopy (EDS) analysis was carried out on the grains of $Nd(Mg_{0.43}Ca_{0.07}Sn_{0.5})O_3$ ceramics that were sintered at 1550 °C for 4 h, as shown in Fig. 3(c). According to the quantitative analysis, which is presented in Table 2, the A and B grains are $Nd(Mg_{0.43}Ca_{0.07}Sn_{0.5})O_3$, and the grain C is $Nd_2Sn_2O_7$.

Fig. 4 shows the apparent densities of $Nd(Mg_{0.5-x}Ca_xSn_{0.5})O_3$ ceramics with different degrees of Ca^{2+} substitution, following sintering at 1450–1600 °C for 4 h. The apparent density was highest for $Nd(Mg_{0.43}Ca_{0.07}Sn_{0.5})O_3$ ceramics that were sintered at 1550 °C with a maximum density of 6.88 g/cm^3. Above 1550 °C, the apparent density decreased. An increase in the apparent density may be caused by a decrease in the number of pores, as shown in Fig. 3. In the series of $Nd(Mg_{0.5-x}Ca_xSn_{0.5})O_3$ ceramics, $Nd(Mg_{0.43}Ca_{0.07}Sn_{0.5})O_3$ ceramics that were sintered at 1550 °C for 4 h had the highest apparent density of 6.88 g/cm^3. Although the weight of a Ca atom is larger than that of a Mg atom, the apparent density of $Nd(Mg_{0.5-x}Ca_xSn_{0.5})O_3$ ceramics that were sintered at 1550 °C for 4 h decreased from 6.88 to 6.83 g/cm^3 as x increased from 0.07 to 0.1. Table 1 shows the relative densities of $Nd(Mg_{0.5-x}Ca_xSn_{0.5})O_3$ ceramics with different degrees of Ca^{2+} substitution, following sintering at 1550 °C for 4 h. In the series of $Nd(Mg_{0.5-x}Ca_xSn_{0.5})O_3$ ceramics, $Nd(Mg_{0.43}Ca_{0.07}Sn_{0.5})O_3$ ceramics had the highest relative density of 97.62%.

Table 1
Tolerance factor, porosity, relative density, and total ionic polarization of $Nd(Mg_{0.5-x}Ca_xSn_{0.5})O_3$ ceramics.

x	Tolerance factor	Porosity (%)	Relative density (%)	Total ionic polarization (Å^3)
0.05	0.8853	0.68	97.26	13.207
0.07	0.8888	0.52	97.62	13.244
0.1	0.8911	0.51	97.13	13.299

Table 2
EDS data for grains of $Nd(Mg_{0.43}Ca_{0.07}Sn_{0.5})O_3$ ceramics sintered at 1550 °C for 4 h.

Atomic element	Nd (%)	Mg (%)	Ca (%)	Sn (%)	O (%)
A	13.25	6.86	1.1	9.29	69.5
B	15.27	6.59	1.74	9.36	67.04
C	18.17	0	0	17.23	64.59

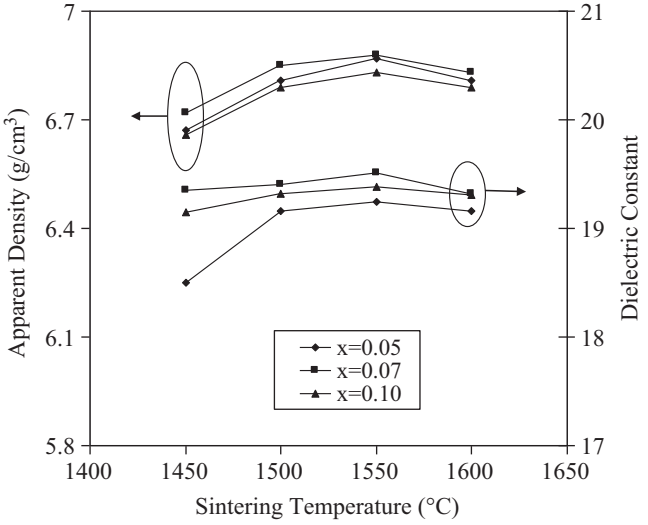

Fig. 4. Apparent densities and dielectric constants of $Nd(Mg_{0.5-x}Ca_xSn_{0.5})O_3$ ceramics with different degrees of Ca^{2+} substitution, following sintering at different temperatures for 4 h.

Fig. 4 also shows the dielectric constants of $Nd(Mg_{0.5-x}Ca_xSn_{0.5})O_3$ ceramics with different degrees of Ca^{2+} substitution, following sintering at 1450–1600 °C for 4 h. $Nd(Mg_{0.43}Ca_{0.07}Sn_{0.5})O_3$ ceramics that were sintered at 1550 °C for 4 h had a dielectric constant of 19.51. The high dielectric constant obtained for $Nd(Mg_{0.43}Ca_{0.07}Sn_{0.5})O_3$ ceramics that were sintered at 1550 °C for 4 h did not depend on a high sintering temperature. The decrease in the dielectric constant is associated with the lower apparent density of the ceramic. A higher apparent density is associated with a lower porosity, and, therefore, a higher dielectric constant. For $Nd(Mg_{0.5-x}Ca_xSn_{0.5})O_3$ ceramics that were sintered at 1550 °C for 4 h, $Nd(Mg_{0.43}Ca_{0.07}Sn_{0.5})O_3$ ceramics had the highest dielectric constant of 19.51. The dielectric constant of $Nd(Mg_{0.5-x}Ca_xSn_{0.5})O_3$ ceramics was affected by many factors, including the ionic polarization and relative density. In the case of ionic polarization, the dielectric constant can be calculated using the Clausius–Mossotti equation

$$\varepsilon_r = \frac{3V_m + 8\pi\alpha_D}{3V_m - 4\pi\alpha_D} \quad (3)$$

where V_m represents the molar volume and α_D is the sum of the ionic polarizabilities of individual ions. The dielectric constant was calculated using Eq. (3) and was found to be an intrinsic material property. Dielectric constants therefore depend on the molar volume and ionic polarization. As indicated by Eq. (3), a smaller molar volume or a larger ionic polarization is associated with a larger dielectric constant. The influence of ionic polarization on dielectric constant is much larger than that of molar volume. Table 1 shows the sum of the ionic polarizations of individual ions of $Nd(Mg_{0.5-x}Ca_xSn_{0.5})O_3$ ceramics with different degrees of Ca^{2+} substitution. The sum of ionic polarizations of individual ions of $Nd(Mg_{0.5-x}Ca_xSn_{0.5})O_3$ increased from 13.207 to 13.299 Å^3 as x increased from 0.05 to 0.1 [15]. However, the dielectric constant of $Nd(Mg_{0.5-x}Ca_xSn_{0.5})O_3$ ceramics decreased as x

increased from 0.07 to 0.1. This is associated with the relative density. The relative densities of $Nd(Mg_{0.5-x}Ca_xSn_{0.5})O_3$ ceramics decreased from 97.62% to 97.13% as x increased from 0.07 to 0.1, as shown in Table 1.

Fig. 5 shows the Qf of $Nd(Mg_{0.5-x}Ca_xSn_{0.5})O_3$ ceramics with different degrees of Ca^{2+} substitution, following sintering at 1450–1600 °C for 4 h. The relationship between the Qf and the sintering temperature of $Nd(Mg_{0.43}Ca_{0.07}Sn_{0.5})O_3$ ceramics was consistent with the relationship between the apparent density and the sintering temperature, because the microwave dielectric loss is affected by many factors, specially intrinsic and extrinsic losses. Intrinsic loss is associated with the vibrational modes of the lattice. Extrinsic loss is associated with density, porosity, second phases, impurities, oxygen vacancies, grain size, and lattice defects [16,17]. Since the Qf of $Nd(Mg_{0.43}Ca_{0.07}Sn_{0.5})O_3$ ceramics was consistent with the variation of the apparent density, the Qf of $Nd(Mg_{0.43}Ca_{0.07}Sn_{0.5})O_3$ ceramics is suggested to be dominated by the apparent density. $Nd(Mg_{0.43}Ca_{0.07}Sn_{0.5})O_3$ ceramics that were sintered at 1550 °C for 4 h had a maximum Qf of 100,400 GHz in the series of $Nd(Mg_{0.5-x}Ca_xSn_{0.5})O_3$ ceramics. The results suggest that the Qf increased by partially substituting Mg^{2+} ions with Ca^{2+} ions. This is associated with the relative density. Since $Nd(Mg_{0.43}Ca_{0.07}Sn_{0.5})O_3$ ceramics have a maximum relative density in the series of $Nd(Mg_{0.5-x}Ca_xSn_{0.5})O_3$ ceramics, the Qf of $Nd(Mg_{0.43}Ca_{0.07}Sn_{0.5})O_3$ ceramics was inferred to be the maximum value.

Fig. 5 shows the τ_f of $Nd(Mg_{0.5-x}Ca_xSn_{0.5})O_3$ ceramics with different degrees of Ca^{2+} substitution, following sintering at 1450–1600 °C for 4 h. The negative τ_f value of $Nd(Mg_{0.5-x}Ca_xSn_{0.5})O_3$ ceramics is associated with the presence of the in-phase and anti-phase tilting of the octahedral [14]. Generally, τ_f is related to the composition, the amount of additive, and the second phases that are present in ceramics. No significant variation occurred for the τ_f of $Nd(Mg_{0.5-x}Ca_xSn_{0.5})O_3$ ceramics over the entire range of sintering temperature. The composition of $Nd(Mg_{0.5-x}Ca_xSn_{0.5})O_3$ ceramics with a fixed amount of Ca^{2+} substitution did not vary with the sintering temperature. $Nd(Mg_{0.43}Ca_{0.07}Sn_{0.5})O_3$ ceramic that was sintered at 1550 °C for 4 h had a τ_f of −57.8 ppm/°C.

Fig. 6 shows the simulation return loss of the hybrid DR antenna with different DR parameters. From the results, the upper resonant frequency decreased from 6.58 to 5.26 GHz as DR height increased from 3 to 7 mm. The upper resonant frequency decreased from 6.36 to 5.22 GHz as DR radius increased from 4 to 6 mm. These results can be explained by using (2). A larger DR height or a larger DR radius is associated with a lower resonant frequency. The upper resonant frequency decreased from 5.89 to 5.42 GHz as DR

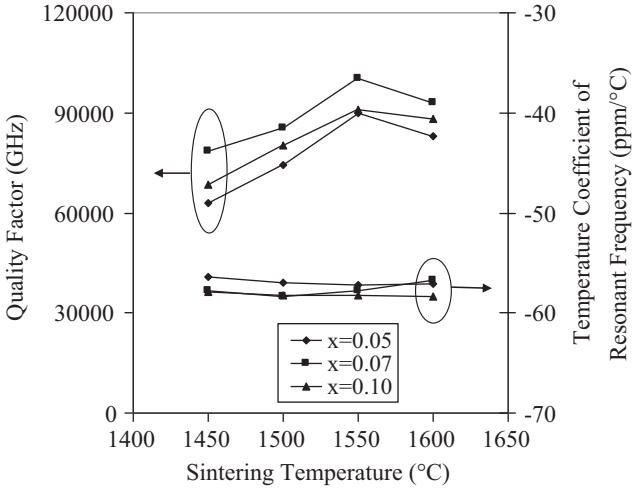

Fig. 5. Qf and τ_f of $Nd(Mg_{0.5-x}Ca_xSn_{0.5})O_3$ ceramics with different degrees of Ca^{2+} substitution, following sintering at different temperatures for 4 h.

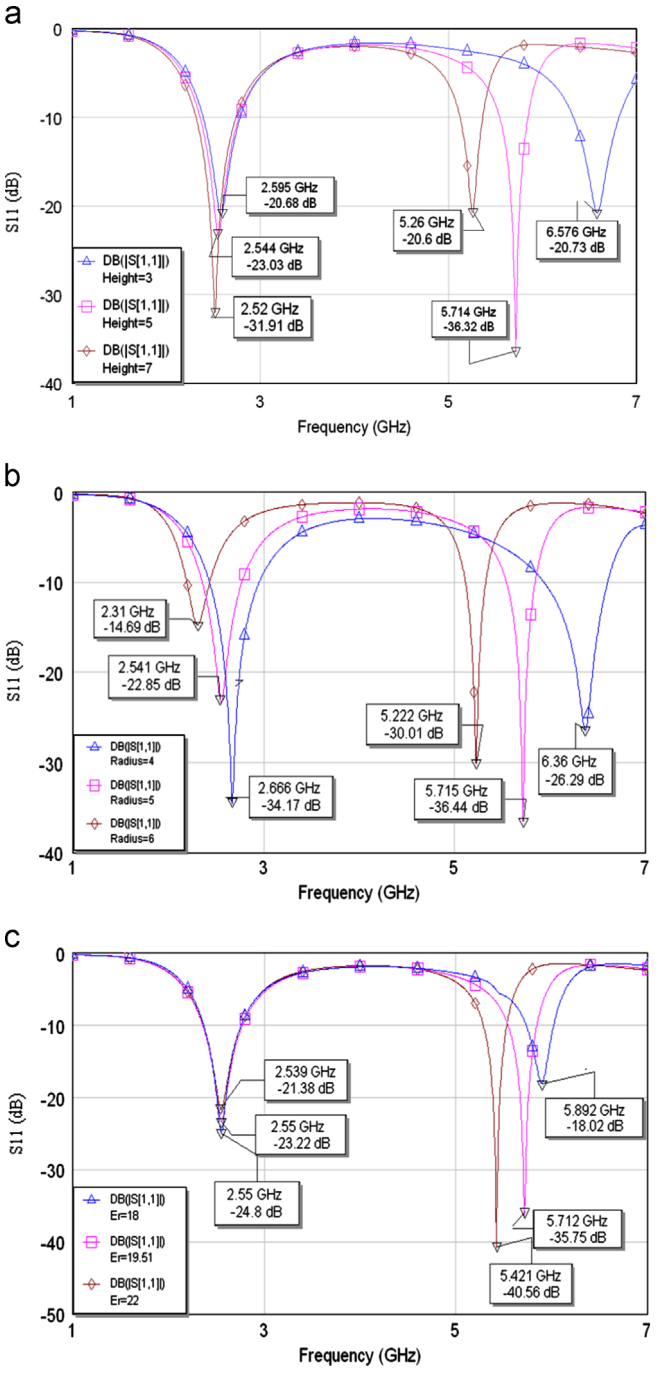

Fig. 6. Simulation return loss of the hybrid DR antenna with different DR parameters of (a) height, (b) radius and (c) dielectric constant.

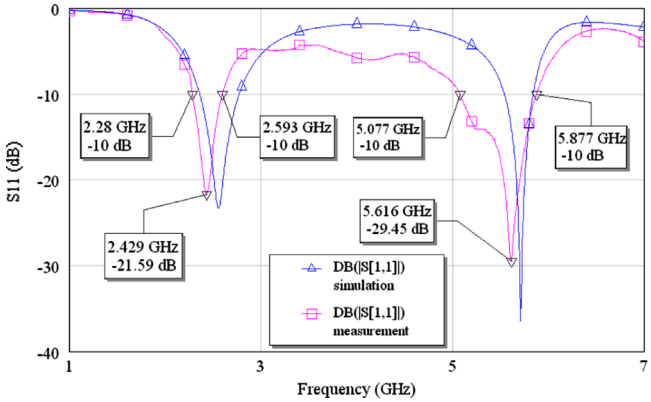

Fig. 7. Measurement and simulation return loss of the hybrid DR antenna.

dielectric constant increased from 18 to 22. As shown in (2), a larger DR dielectric constant enabled the lower resonant frequency. The upper resonant frequency of the hybrid DR antenna demonstrated to be dominated by the DR parameters.

Fig. 7 shows the measurement and simulation return loss of the hybrid DR antenna. The measurement resonant frequency was close to the simulation resonant frequency. The return losses were −22, and −29 dB at 2.43 and 5.62 GHz, respectively. There was a 10 dB return loss bandwidth of 313 MHz (2280–2593 MHz) and 800 MHz (5077–5877 MHz). Alternatively, the antenna had a 10 dB S_{11} bandwidth of 12.5% and 14.2%, which covered the required bandwidth 2400–2484 MHz, 5150–5350 MHz, and 5725–5825 MHz, simultaneously. The bandwidth at the higher resonant frequency, associated with the cylindrical DR with a high dielectric constant, was larger than the typical value of 6–12% of the conventional DR antenna using DR with dielectric constant around 10 [9–11].

4. Conclusions

The effects of Ca^{2+} substitution and sintering temperature on the microwave dielectric properties of $Nd(Mg_{0.5-x}Ca_xSn_{0.5})O_3$ ceramics were studied. Substituting Mg^{2+} ions with Ca^{2+} ions was found to improve the microwave dielectric properties of $Nd(Mg_{0.5-x}Ca_xSn_{0.5})O_3$ ceramics. $Nd(Mg_{0.43}Ca_{0.07}Sn_{0.5})O_3$ ceramics that were sintered at 1550 °C for 4 h had an apparent density of 6.88 g/cm^3, a dielectric constant of 19.51, a Qf of 100,400 GHz, and a τ_f of −57.8 ppm/°C. The density affected the dielectric constant and the Qf of $Nd(Mg_{0.5-x}Ca_xSn_{0.5})O_3$ ceramics. The dielectric constant of $Nd(Mg_{0.5-x}Ca_xSn_{0.5})O_3$ ceramics was also dependent on the ionic polarization. A hybrid DR antenna using DR with high dielectric constant, was successfully manufactured. The structure of the proposed antenna was simple and easily manufactured. The return losses were −22 and −29 dB at 2.43 and 5.62 GHz, respectively. The corresponding −10 dB S_{11} bandwidths were 12.5% and 14.2% at 2.43 and 5.62 GHz, respectively. The −10 dB S_{11} bandwidth of the proposed antenna covered the ISM, UNII, and HIPERLAN bands.

Acknowledgments

This work was supported by the National Science Council of Taiwan under Grant NSC 101-2221-E-262-009-.

References

[1] Y.C. Chen, Microwave dielectric properties of $(Mg_{(1-x)}Co_x)_2SnO_4$ ceramics for application in dual-band inverted-E-shaped monopole antenna, IEEE Transactions on Ultrasonics Ferroelectrics and Frequency Control 58 (2011) 2531–2538.
[2] Y.C. Chen, R.J. Tsai, Effect of sintering temperature and time on microwave dielectric properties of $Nd(Mg_{0.5}Sn_{0.5})O_3$ ceramics, Materials Chemistry and Physics 129 (2011) 116–120.
[3] Y.C. Chen, R.J. Tsai, Y.N. Wang, Dielectric properties of B_2O_3-doped $Nd(Mg_{1/2}Sn_{1/2})O_3$ ceramics at microwave frequencies, Ferroelectrics 396 (2010) 104–112.
[4] Y.C. Chen, C.Y. Wu, Effect of Sr substitution on microwave dielectric properties of $Nd(Mg_{0.5}Sn_{0.5})O_3$ ceramics, Ceramics International 39 (2013) 1877–1883.
[5] Y.C. Chen, K.C. Chang, S.L. Yao, Improved microwave dielectric properties of $Nd(Mg_{0.5}Sn_{0.5})O_3$ ceramics by substituting Mg^{2+} with Zn^{2+}, Ceramics International 38 (2012) 5377–5383.
[6] Y.C. Chen, R.J. Tsai, C.Y. Wu, Microwave dielectric properties and microstructures of $Nd(Mg_{0.5}Sn_{0.5-x}Ti_x)O_3$ ceramics, Ceramics International 38 (2012) 2927–2934.
[7] R.D. Shannon, Revised effective ionic radii and systematic studies of interatomic distances in halides and chalcogenides, Acta Crystallographica A 32 (1976) 751–767.
[8] S.A. Long, M. McAllister, L.C. Shen, The resonant cylindrical dielectric cavity antenna, IEEE Transactions on Antennas and Propagation 31 (1983) 406–412.
[9] R.K. Mongia, A. Ittipiboon, M. Cuhaci, Low profile dielectric resonator antennas using a very high permittivity material, Electronics Letters 30 (1994) 1362–1363.
[10] K.M. Luk, M.T. Lee, K.W. Leung, E.K.N. Yung, Technique for improving coupling between microstrip line and dielectric resonator antenna, Electronics Letters 35 (1999) 357–358.
[11] Y.X. Guo, K.M. Luk, On improving coupling between a coplanar waveguide feed and a dielectric resonator antenna, IEEE Transactions on Antennas and Propagation 51 (2003) 2144–2146.
[12] B.W. Hakki, P.D. Coleman, A dielectric resonator method of measuring inductive capacities in the millimeter range, IEEE Transactions on Microwave Theory and Techniques 8 (1960) 402–410.
[13] A.M. Glazer, Simple ways of determining perovskite structures, Acta Crystallographica A 31 (1975) 756–762.
[14] I.M. Reaney, E.L. Collea, N. Setter, Dielectric and structural characteristics of Ba- and Sr-based complex perovskites as a function of tolerance factor, Japanese Journal of Applied Physics 33 (1994) 3984–3990.
[15] R.D. Shannon, Dielectric polarizabilities of ions in oxides and fluorides, Journal of Applied Physics 73 (1993) 348–366.
[16] B.D. Silverman, Microwave absorption in cubic strontium titanate, Physical Review 125 (1962) 1921–1930.
[17] W.S. Kim, T.H. Hong, E.S. Kim, K.H. Yoon, Microwave dielectric properties and far infrared reflectivity spectra of the $(Zr_{0.8}Sn_{0.2})TiO_4$ ceramics with additives, Japanese Journal of Applied Physics 37 (1998) 3567–3571.